IOP Conf. Series: Journal of Physics: Conf. Series **871** (2017) 012043 doi:10.1088/1742-6596/871/1/012043

Critical current density of YBCO films with different configurations of columnar defects in longitudinal magnetic field

T Sueyoshi[1], Y Iwanaga[1], T Kai[1], T Izumi[1], T Fujiyoshi[1] and N Ishikawa[2]

[1] Department of Computer Science and Electrical Engineering, Kumamoto University, 2-39-1 Kurokami, Chuo-ku, Kumamoto 860-8555, Japan
[2] Japan Atomic Energy Agency (JAEA), Tokai-mura, Ibaraki 319-1195, Japan

E-mail: tetsu@cs.kumamoto-u.ac.jp

Abstract. Critical current density (J_c) properties in longitudinal magnetic fields were investigated for $YBa_2Cu_3O_y$ thin films with columnar defects (CDs), where different configurations of CDs were systematically installed into the films by using heavy-ion irradiation: a parallel configuration of CDs aligned along the *c*-axis and two bimodal splay configurations composed of CDs crossing at $\pm\theta_i$ relative to the *c*-axis, where the splay plane defined by the two irradiation angles is perpendicular or parallel to the transport current direction. The unirradiated film under the longitudinal magnetic field shows a J_c peak in the magnetic field dependence of J_c, which is 1.1 times higher than the self-field J_c. For the irradiated films with the parallel CD configuration, on the other hand, the J_c is lower than that for the unirradiated film in all magnetic fields and the value of J_c decreases with increasing CD density. Such degradation effect by CDs under longitudinal magnetic field was observed even for the bimodal splay configurations. These results are attributed to local meandering of current flow induced by CDs extending through the film thickness, which deteriorates the force-free condition.

1. Introduction

In recent years, superconducting applications contributing to high energy efficiency and low-carbon energy have been actively developed, since $REBa_2Cu_3O_y$ (REBCO, RE: Rare Earth element) coated conductors are commercially available now. One of the applications peculiar to superconducting tapes such as the coated conductors is a force-free cable [1, 2]. This utilizes an increment of critical current density J_c in a magnetic field parallel to the transport current, i.e. the so-called longitudinal magnetic field effect, where no Lorentz force works on flux lines, namely the force-free state is induced [3-5]. The flux lines under the force-free state, on the other hand, receive a force-free torque resulting from current-induced rotational shear distortion of flux lines [6]. Hence, flux pinning for the force-free torque (i.e. pinning torque) is one of the key issues to improve J_c even in the longitudinal magnetic field: there is still room for improvement in J_c under the longitudinal magnetic field by additional pinning centers (PCs).

The improvement of J_c in the longitudinal magnetic field has been experimentally observed by introducing additional PCs: neutron irradiation defects in Nb_3Sn tapes [4], $BaHafO_3$ nano-particles in

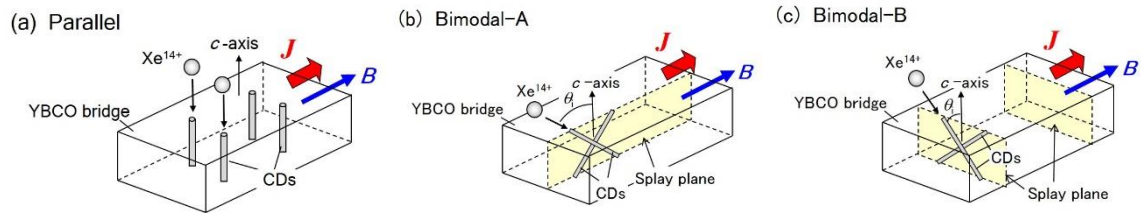

Figure 1. Illustration of various configurations of CDs installed into YBCO films by heavy-ion irradiation: (a) parallel, (b) bimodal-A, and (c) bimodal-B.

SmBCO films [7, 8] and Y_2O_3 nano-particles in YBCO films [9]. Common feature to these PCs effective for the longitudinal magnetic field effect is spherical shape, i.e. random PCs. In a magnetic field perpendicular to transport current (maximum Lorentz force configuration), on the other hand, linear defects such as dislocations [10], nano-rods [11] and columnar defects (CDs) [12], are most effective to immobilize flux lines in high-T_c superconductors. Moreover, the value of J_c in any direction can be customized by the dispersion in direction of linear defects [13]. Despite of such high performance pinning, there has been little or no research for the influence of linear defects on the longitudinal magnetic field effect so far.

In this work, we systematically explored the influence of CDs on J_c properties of YBCO thin films in the longitudinal magnetic field, where various configurations of CDs were installed into the films by using heavy-ion irradiation, as shown in figure 1: a parallel configurations of CDs aligned along the *c*-axis with different densities of CDs, and two bimodal splay configurations composed of CDs crossing at $\pm\theta_i$ relative to the *c*-axis, where the splay plane defined by the two irradiation angles is parallel (bimodal-A) or perpendicular (bimodal-B) to the transport current direction.

2. Experimental details

The samples used in this work were *c*-axis oriented YBCO thin films, which were fabricated by a pulsed laser deposition (PLD) technique on the (100) surface of $SrTiO_3$ substrates. The thickness of the films was about 300 nm. The films were patterned in a bridge geometry with about 40 μm width and 1 mm length before irradiation.

After the patterning process, the samples were irradiated with 200 MeV Xe ions at the tandem accelerator of JAEA in Tokai, Japan. To install various configurations of crossed CDs into the films, the incident angle of the ion beam was tilted off the *c*-axis by $\pm\theta_i$ in two geometries where a splay plane defined by the two irradiation angles is perpendicular (bimodal-A) or parallel (bimodal-B) to the bridge direction (current flow direction), as shown in figure 1. The electronic stopping power S_e for the irradiation is about 28 keV/nm at the surface of the sample. This creates continuous CDs of 5 ~ 9 nm diameter along the incident ion beam directions, which were confirmed by a cross-sectional transmission electron microscopy image in our previous work [14]. Table 1 lists the specifications of the samples in this work. The matching field B_ϕ, which corresponds to the planar density of CDs, is defined with respect to each irradiation direction. For the bimodal configurations, the fluence for each irradiation direction is half the total one.

Table 1 Samples in this work.

Sample	Configuration of CDs	θ_i	B_ϕ [T]	T_c [K]	J_{c0} [MA/cm^2]
Pure	-	-	-	89.3	2.21
PR05	Parallel	0°	0.5	89.5	3.49
PR10	Parallel	0°	1.0	89.1	2.68
BA80	Bimodal-A	±80°	1.0	89.2	3.62
BB45	Bimodal-B	±45°	1.5	89.2	2.79
BB85	Bimodal-B	±85°	1.5	89.2	2.39

Transport properties were measured using a four-probe method, The value of J_c was determined using a criterion of electrical field, 1 μV/cm. For the J_c measurements as a function of applied magnetic field direction in maximum Lorentz force configuration, the transport current was applied always in the direction perpendicular to the magnetic field. In order to evaluate the J_c properties in longitudinal magnetic field, on the other hand, the magnetic field was applied parallel to the bridge direction (i.e. current flow direction).

3. Results and discussion

Firstly, we investigated the angular dependence of J_c under the maximum Lorentz force configuration in order to check the effectiveness of flux pinning by various configurations of CDs. Figure 2a shows the angular dependence of J_c for the unirradiated- and the irradiated-samples with $B_\phi = 1$ T, where θ is the angle between the magnetic field and the c-axis of the YBCO films. The unirradiated sample indicates a smooth angular dependence of J_c exhibiting a minimum at $B \parallel c$, which is typical of uncorrelated flux pinning due to naturally occurring growth defects [15]. For the parallel CD configuration, by contrast, a large enhancement of J_c centered at $B \parallel c$ can be observed, although the J_c was slightly reduced around $B \parallel ab$ compared to the unirradiated sample. This means that CDs with $\theta_i = 0°$ effectively work as c-axis correlated PCs. The bimodal-A configuration with $\theta_i = \pm 80°$, on the other hand, shows an overall shift upward in J_c compared to the unirradiated sample, where the angular behavior of J_c consists of a broad peak centered at $B \parallel ab$ and an additional peak at $B \parallel ab$. The J_c behavior is typical of the random pinning, as well as the unirradiated sample. For the bimodal-A configuration with the large CD crossing angle, the CDs provide uncorrelated pinning instead of correlated pinning, because flux lines interact with the largely inclined CDs at the intersection points in any direction of magnetic field [16].

In figure 2b, the angular dependence of J_c is represented for the bimodal-B configurations with $\theta_i = \pm 45°$ and $\pm 85°$, in comparison with the unirradiated sample. For $\theta_i = \pm 45°$, a large enhancement of J_c can be observed in a wide angular range, resulting in not so much a peak as a plateau-like behavior. The plateau-structure of the J_c centered at $\theta = 0°$ is attributed to the uncorrelated pinning by crossed CDs with $\theta_i = \pm 45°$, which provides strong pinning around $B \parallel c$ for low magnetic field [14]. The J_c of the bimodal-B configuration with $\theta_i = \pm 85°$, in contrast, falls below that of the unirradiated samples around $B \parallel c$. In the vicinity of $B \parallel ab$, on the other hand, a pronounced J_c peak emerges for $\theta_i = \pm 85°$, whereas the J_c at $B \parallel ab$ deteriorates for most of the other CD configurations: the CDs with $\theta_i = \pm 85°$ provide the extremely effective flux pinning for $B \parallel ab$.

From the above results, it is shown that CDs work as effective PCs in various directions of magnetic field depending on the configuration of CDs under the maximum Lorentz force

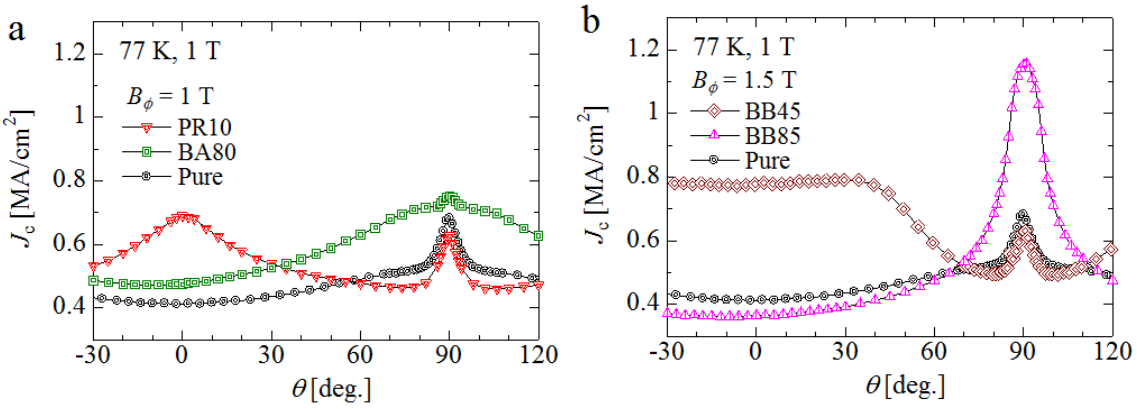

Figure 2. Angular dependence of J_c for YBCO films with different CD configurations under the maximum Lorentz force configuration: (a) parallel and bimodal-A, and (b) bimodal-B configurations, compared with an unirradiated sample.

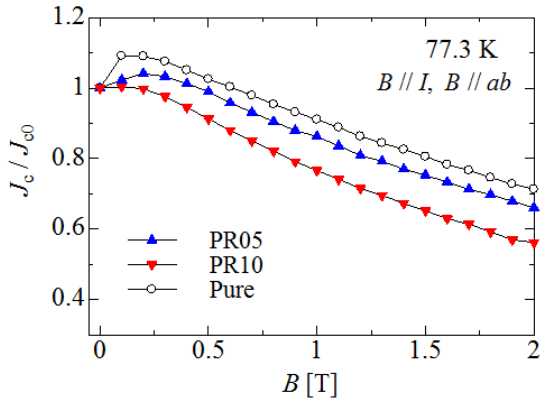

Figure 3. Magnetic field dependence of normalized J_c for YBCO films including a parallel CD configuration in longitudinal magnetic fields.

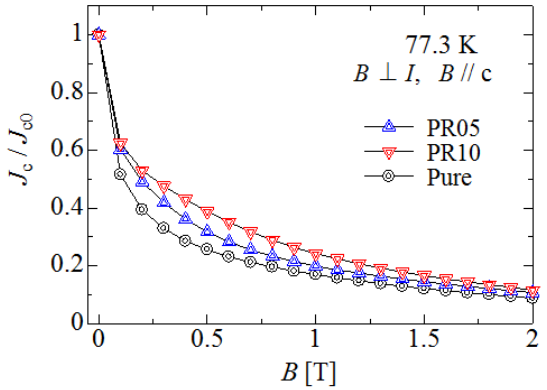

Figure 4. Magnetic field dependence of normalized J_c for YBCO films including a parallel CD configuration in transverse magnetic fields.

configuration. Next, we discuss the influence of these configurations of CDs on J_c under the force-free configuration. Figure 3 shows the magnetic field dependence of normalized J_c by the self-field critical current density J_{c0} for the parallel CD configurations with B_ϕ = 0.5 T and 1 T in the longitudinal magnetic field, in comparison with the unirradiated film. For the unirradiated sample, the J_c becomes higher than the J_{c0} up to 0.7 T, leading to the peak structure. The peak value of J_c near 0.2 T was about 10 % higher than that of J_{c0}, which is about same as the case of a SmBCO film with $BaHfO_3$ nanoparticles [7, 8]. This suggests the naturally occurring growth defects provide effective flux pinning for the unirradiated film. For the irradiated films, on the other hand, the J_c is lower than that for the unirradiated film in all magnetic fields. Furthermore, the value of J_c decreases with increasing CD density, although the J_c increases with increasing CD density at $B \parallel c$ under the maximum Lorentz force configuration, as shown in figure 4. For the increase in J_c by the longitudinal magnetic field effect, the current flow direction needs to be parallel to the magnetic field direction. The CDs, however, would disturb the current flow direction, since the CDs perpendicular to the current direction extend through the film thickness: the parallel relation between the current and the magnetic field is locally loosened by the CDs. The high density of CDs increases the degree of the meandering of the current flow. Therefore, the introduction of CDs with θ_i = 0° reduces the J_c in the longitudinal magnetic field.

Figure 5 shows a comparison of J_c between the parallel and the bimodal-A configurations under the longitudinal magnetic field. The bimodal-A configuration indicates the lowest J_c of the three films, although the J_c of the bimodal-A configuration is the highest at $B \parallel ab$ under the maximum Lorentz force configuration as shown in figure 2(a). This is attributed to larger meandering of current flow due to the inclination of CDs: the diameter of CDs in the *ab*-plane is proportional to $1/\cos\theta_i$, so that the current more meanderingly flows along the *ab*-plane. It should be noted that the J_c of the bimodal-A configuration is the same as or a little higher than that of the parallel one in low magnetic field up to 0.1 T. This suggests that the crossed CDs extending to the magnetic field direction slightly contribute to the flux pinning in a lower magnetic field, because flux lines are subjected not only to the force-free torque but also to the Lorentz force directed to the thickness direction due to the distortion of flux lines by the self-field [8].

Figure 6 represents the magnetic field dependence of J_c in the longitudinal magnetic field for bimodal-B configurations with θ_i = ±45° and ±85°. The value of J_c decreases with increasing CD crossing angle. In particular, the sample with θ_i = ±85° indicates the rapid reduction of J_c without showing a peak of J_c, although the J_c for θ_i = ±85° is the highest of all the films at $B \parallel ab$ under the

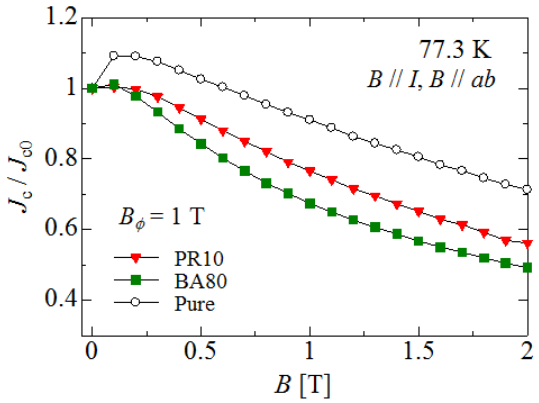

Figure 5. Magnetic field dependence of normalized J_c for YBCO films with the parallel and the bimodal-A configuration in longitudinal magnetic fields.

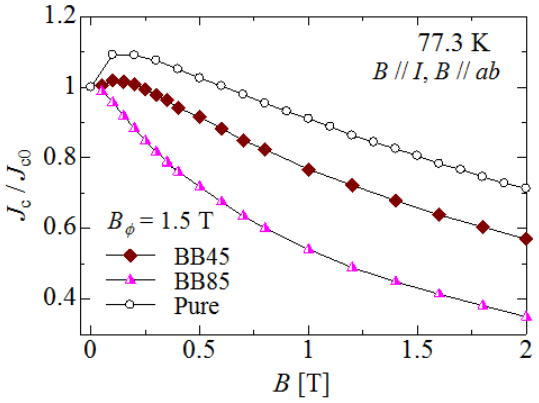

Figure 6. Magnetic field dependence of normalized J_c for YBCO films with the bimodal-B configuration in longitudinal magnetic fields.

maximum Lorentz force configuration as shown in figure 2b. The meandering of the current, which reduces the longitudinal magnetic field effect, is more frequent with increasing CD crossing angle, since the crossed CDs is always perpendicular to the current direction for the bimodal-B configurations and the inclined CDs extending through the sample thickness becomes longer as $1/\cos\theta_i$.

From the above results, it is shown that any configuration of CDs provides the deterioration effect for the flux pinning in longitudinal magnetic fields. One reason for the deterioration effect is that CDs extending through the film thickness induces local meandering of the current flow so as to loosen the parallel relation between the current and the magnetic field. It was reported that weak links of grain boundaries in high-T_c superconductors induce the local meandering of current flow, leading to the reduction of the longitudinal magnetic field effect [17]. Another possible reason is that CDs exhibiting a preferential direction for flux pinning cannot provide the effective pinning torque against the rotational torque, i.e. the force-free torque. In contrast, the uncorrelated PCs such as nano-particles could act as effective PCs in the longitudinal magnetic field, because the uncorrelated PCs provide the isotropic pinning against any orientations of magnetic field. In fact, the effectiveness of nano-particles for the flux pinning in the longitudinal magnetic field has been reported for SmBCO films including $BaHfO_3$ nano-particles [7, 8] and YBCO films with Y_2O_3 nano-particles [9].

4. Conclusions

We systematically investigated the influence of CD configurations on J_c in a longitudinal magnetic field, by using heavy-ion irradiation. All of the CD configurations deteriorated the J_c properties in the longitudinal magnetic field in comparison with the unirradiated sample, although the CDs acted as effective PCs in different directions of magnetic field depending on the configuration of CDs under the maximum Lorentz force configuration: the value of J_c decreased with increasing CD density and/or CD crossing angle in the longitudinal magnetic field. The installation of CDs extending through the film thickness induces local meandering of the current flow over the thickness direction, resulting in larger suppression of the longitudinal magnetic field effect.

Acknowledgements

This work was supported by KAKENHI (25234567 and 16K06269) from the Japan Society for the Promotion of Science and was partly performed under the Common-Use Facility Program of JAEA.

References

[1] Matsushita T, Kiuchi M and Otabe E S, 2012 *Supercond. Sci. Technol.* **25** 125009
[2] Vyatkin V S, Kiuchi M, Otabe E S, Ohya M and Matsushita T, 2015 *Supercond. Sci. Technol.*

28 015011
[3] Bychkov Yu F, Vereshchagin V G, Zuev M T, Karasik V R, Kurganov G B and Mal'tsev V A, 1969 *JETP Lett.* **9** 404
[4] Cullen G W and Novak R L, 1964 *Appl. Phys. Lett.* **4** 147
[5] Maiorov B, Jia Q X, Zhou H, Wang H, Li Y, Kursunovic A, MacManus-Driscoll J L, Haugan T J, Barnes P N, Foltyn S R and Civale L, 2007 *IEEE Trans. Appl. Supercond.* **17** 3697
[6] Matsushita T, 1985 *J. Phys. Soc. Jpn.* **54** 1054
[7] Tsuruta A, Watanabe S, Ichino and Y, Yoshida Y, 2014 *Jpn. J. Appl. Phys.* **53** 078003
[8] Sugihara K, Ichino Y and Yoshida Y, 2015 *Supercond. Sci. Technol.* **28** 104004
[9] Kido R, Kiuchi M, Otabe E S, Matsushita T, Jha A K and Matsumoto K, 2016 *Phys. Proc.* **81** 117
[10] Lowndes D H, Christen D K, Klabunde C E, Wang Z L, Kroeger D M, Budai J D, Zhu S and Norton D P, 1995 *Phys. Rev. Lett.* **74** 2355
[11] Macmanus-Driscoll J L, Foltyn S R, Jia Q X, Wang H, Serquis A, Civale L, Maiorov B, Hawley M E, Maley M P and Peterson D E 2004 *Nature Mater.* **3** 439
[12] Civale L, Marwick A D, Worthington T K, Kirk M A, Thompson J R, Krusin-Elbaum L, Sun Y, Clem J R and Holtzberg F 1991 *Phys. Rev. Lett.* **67** 648
[13] Maiorov B, Baily S A, Zhou H, Ugurlu O, Kennison J A, Dowden P C, Holesinger T G, Foltyn S R and Civale L 2009 *Nature Mater.* **8** 398
[14] Sueyoshi T, Sogo T, Nishimura T, Fujiyoshi T, Mitsugi F, Ikegami T, Awaji S, Watanabe K, Ichinose A and Ishikawa N 2016 *Supercond. Sci. Technol.* **29** 065023
[15] Civale L, Maiorov B, Serquis A, Willis J O, Coulter J Y, Wang H, Jia Q X, Arendt P N, MacManus-Driscoll J L, Maley M P and Foltyn S R 2004 *Appl. Phys. Lett.* **84** 2121
[16] Furuki Y, Sueyoshi T, Kai T, Iwanaga Y, Fujiyoshi T and Ishikawa N 2015 *Physica C* **518** 58
[17] Safar H, Coulter J Y, Maley M P, Foltyn S, Arendt P, Wu X D and Willis J O 1995 *Phys. Rev. B* **52** R9875